Cell Metabolism
Article

Sirt1 Extends Life Span and Delays Aging in Mice through the Regulation of Nk2 Homeobox 1 in the DMH and LH

Akiko Satoh,[1] Cynthia S. Brace,[1] Nick Rensing,[2] Paul Cliften,[3] David F. Wozniak,[4,5] Erik D. Herzog,[5,6] Kelvin A. Yamada,[2] and Shin-ichiro Imai[1,*]
[1]Department of Developmental Biology
[2]Department of Neurology
[3]Department of Genetics
[4]Department of Psychiatry
[5]Hope Center for Neurological Disorders
Washington University School of Medicine, St. Louis, MO 63110, USA
[6]Department of Biology, Washington University, St. Louis, MO 63130, USA
*Correspondence: imaishin@wustl.edu
http://dx.doi.org/10.1016/j.cmet.2013.07.013

SUMMARY

The mammalian Sir2 ortholog Sirt1 plays an important role in metabolic regulation. However, the role of Sirt1 in the regulation of aging and longevity is still controversial. Here we demonstrate that brain-specific *Sirt1*-overexpressing (BRASTO) transgenic mice show significant life span extension in both males and females, and aged BRASTO mice exhibit phenotypes consistent with a delay in aging. These phenotypes are mediated by enhanced neural activity specifically in the dorsomedial and lateral hypothalamic nuclei (DMH and LH, respectively), through increased orexin type 2 receptor (*Ox2r*) expression. We identified Nk2 homeobox 1 (Nkx2-1) as a partner of Sirt1 that upregulates *Ox2r* transcription and colocalizes with Sirt1 in the DMH and LH. DMH/LH-specific knockdown of *Sirt1*, *Nkx2-1*, or *Ox2r* and DMH-specific *Sirt1* overexpression further support the role of Sirt1/Nkx2-1/Ox2r-mediated signaling for longevity-associated phenotypes. Our findings indicate the importance of DMH/LH-predominant Sirt1 activity in the regulation of aging and longevity in mammals.

INTRODUCTION

Over the past decade, a number of evolutionarily conserved regulators and signaling pathways have been identified for the control of aging and longevity. These regulators and signaling pathways, including insulin/insulin-like growth factor 1 (IGF-1) signaling (IIS) (Kenyon, 2010), mammalian target of rapamycin (mTOR) signaling (Zoncu et al., 2011), and NAD-dependent sirtuins (Haigis and Sinclair, 2010), provide excellent probes to dissect complex hierarchical mechanisms that affect the aging process and longevity in each model organism. Recent studies in worms and flies have also suggested that systemic interplay between multiple tissues regulates aging and longevity (Demontis and Perrimon, 2010; Durieux et al., 2011). In mammals, however, the complexity of tissue interplay is multiplied, and a blueprint for a systemic network regulating aging and longevity still remains elusive. Most recently, it has been shown that hypothalamic NF-κB signaling plays a critical role in the regulation of systemic aging via immune-neuroendocrine integration in mice, implicating the importance of the hypothalamus in systemic aging/longevity control in mammals (Zhang et al., 2013). Indeed, the hypothalamus communicates with multiple peripheral tissues via hormonal and neural networks and coordinates metabolic and behavioral responses to nutritional and environmental stimuli. For instance, neurons producing growth hormone (GH)-releasing hormone and somatostatin that stimulate and inhibit GH release in the anterior pituitary gland, respectively, are localized in the hypothalamus. The growth hormone (GH)/IGF-1 axis, which regulates somatic growth, metabolism, and tissue repair, has been well established to control aging and longevity in mammals (Bartke, 2011). Therefore, this particular tissue in the brain appears to function as a critical juncture for the coordination of metabolic signaling and aging/longevity control in mammals.

Sir2 (silent information regulator 2) family proteins, now called "sirtuins," have been demonstrated to coordinate metabolic responses to changes in nutritional availability and maintain physiological homeostasis in mammals (Haigis and Sinclair, 2010). These functions of sirtuins are ascribed to their unique NAD-dependent enzymatic activities (Feldman et al., 2012), placing sirtuins at the perfect position to integrate energy metabolism information into many other biological regulations. In particular, the mammalian Sir2 ortholog Sirt1 plays a critical role for the regulation of metabolic responses in multiple tissues, including the liver, skeletal muscle, adipose tissue, and brain, through its deacetylase activity (Haigis and Sinclair, 2010). Sirt1 also plays a role in the regulation of phenotypes induced by diet restriction (DR), a diet regimen that delays aging and extends life span in a wide variety of organisms (Haigis and Sinclair, 2010). Whereas the whole-body and brain-specific *Sirt1* knockout mice fail to respond to DR (Chen et al., 2005; Cohen et al., 2009; Kume

et al., 2010; Satoh et al., 2010), *Sirt1*-overexpressing transgenic mice display phenotypes similar to DR mice (Bordone et al., 2007) or preventive effects on metabolic complications caused by high-fat diet and aging (Banks et al., 2008; Pfluger et al., 2008). However, whole-body *Sirt1*-overexpressing mice fail to show life span extension (Herranz et al., 2010). Additionally, the importance of Sir2 orthologs for aging/longevity control in worms and flies has recently been called into question (Burnett et al., 2011). Therefore, whether Sirt1 plays an important role in the regulation of aging and longevity in mammals has been a big controversy in the field of aging research.

We have previously demonstrated that hypothalamic Sirt1 functions as a key mediator of the neurobehavioral adaptive response to DR (Satoh et al., 2010). DR significantly increases Sirt1 protein levels and induces neural activation in the dorsomedial and lateral hypothalamic nuclei (DMH and LH, respectively). Interestingly, brain-specific *Sirt1*-overexpressing (BRASTO) transgenic mice exhibit significantly enhanced neural activity specifically in the DMH and LH and augmented neurobehavioral responses to diet-restricting conditions, whereas these responses are abrogated in *Sirt1*-deficient mice (Satoh et al., 2010). Given that DR significantly delays the aging process and extends life span in a variety of animal species, we hypothesized that BRASTO mice might show significant beneficial effects on the aging process and even longevity. Here we show that BRASTO mice exhibit a significant delay in the aging process and extension of life span in both males and females. Sirt1-dependent neural activation in the DMH and LH protects against age-related declines in skeletal muscle mitochondrial function, physical activity, body temperature, oxygen consumption, and quality of sleep. Sirt1 and its partner Nk2 homeobox 1 (Nkx2-1) regulate these physiological functions through the upregulation of orexin type 2 receptor (Ox2r) expression in the DMH and LH, and their colocalization identifies a specific subset of neurons in these hypothalamic regions. Our findings provide critical insight into the importance of hypothalamic Sirt1 and its role in the systemic regulation of tissue communication, aging, and longevity in mammals.

RESULTS

BRASTO Mice Show Significant Life Span Extension and Delay in the Aging Process Compared to Control Mice

Our previous study on the role of hypothalamic Sirt1 in the central adaptive response to low energy intake such as DR provoked a hypothesis that hypothalamic Sirt1 might play an important role in the regulation of the aging process and possibly longevity under an ad libitum regular chow-fed condition in mammals (Satoh et al., 2010). To address this hypothesis, we examined the life span and the age-associated physiological changes in male and female mice overexpressing Sirt1 in the brain (BRASTO, line 10). This particular line has a Sirt1 expression profile in the hypothalamus very similar to that induced by DR in wild-type mice, namely the DMH/LH-predominant increase in Sirt1 expression (Satoh et al., 2010). To avoid any unexpected genetic effects on aging and longevity in this line, we conducted whole-genome sequencing and confirmed that there were no hidden mutations or deletions in this transgenic line 10 (data not shown). This whole-genome analysis also allowed us to identify the integration site of the transgene (see Figure S1A online). Approximately 14 tandem copies of the transgene were integrated into a long intron of the *Ccdc7* gene on chromosome 8. This gene, whose function is unknown, had no detectable expression in most peripheral tissues and the brain, including the soleus muscle, cortex, and hypothalamus, in both males and females (Wang et al., 2009; data not shown). The only exception was testis in males, and one of the splicing variants showed a decrease in its expression only in testis from BRASTO males compared to controls (Figure S1B). No microRNAs were predicted at or around this integration site. Therefore, based on the whole-genome and expression analyses, there is no evidence for any additional genetic changes that systemically affect both males and females in this transgenic line.

Importantly, when fed regular chow ad libitum, both BRASTO females and BRASTO males showed significant life span extension. BRASTO females showed ~16% extension for median life span (control 799 days versus BRASTO 930 days, log rank test, $\chi^2 = 12.2$, df = 1, $p < 0.001$) and statistically significant extension for maximal life span (10% oldest control 1,015 ± 15 days versus BRASTO 1,076 ± 10 days, t test, $p < 0.05$; 20% oldest control 973 ± 15 days versus BRASTO 1,056 ± 10 days, t test, $p < 0.001$) (Figure 1A and Figure S1C). BRASTO males showed ~9% extension in median life span (control 849 days versus BRASTO 926 days, log rank test, $\chi^2 = 5.9$, df = 1, $p = 0.015$) and a trend of maximal life span extension (10% oldest control 1,066 ± 15 days versus BRASTO 1,105 ± 9 days, not significant; 20% oldest control 1,034 ± 15 days versus BRASTO 1,084 ± 9 days, t test, $p < 0.05$). Combined sex results showed ~11% extension for median life span (control 835 days versus BRASTO 926 days; log rank test, $\chi^2 = 14.8$, df = 1, $p < 0.001$) and statistically significant maximal life span extension (10% oldest control 1,049 ± 13 days versus BRASTO 1,092 ± 8 days, t test, $p < 0.001$; 20% oldest 1,003 ± 13 days versus BRASTO 1,070 ± 8 days, t test, $p < 0.001$).

We also assessed age-associated mortality and cancer-dependent death incidence in BRASTO mice. Both BRASTO females and males, as well as combined results, showed significant delays in age-associated mortality, whereas the slopes of age-associated mortality change, which mathematically defines the rate of aging (de Magalhães et al., 2005), did not differ between BRASTO and control mice (Figure 1B). We also observed a similar delay in cancer-dependent death incidence, whereas the slopes of accumulating death incidents and the spectrum of cancers did not differ between BRASTO and control mice (Figures 1C and 1D). These results suggest that the onset of age-associated physiological decline is delayed without affecting the rate of aging in BRASTO mice.

Aged BRASTO Mice Display Significant Enhancement in Physical Activity, Body Temperature, Oxygen Consumption, and Quality of Sleep Compared to Age-Matched Control Mice

As previously reported at 5 months of age (Satoh et al., 2010), BRASTO and control mice at 20 months of age exhibited no significant differences in body weight; fed and fasted blood glucose, insulin, and lipid levels; and glucose and insulin tolerance (Figures S2A–S2H). Nonetheless, BRASTO mice at 20 months of age showed significantly higher physical activity

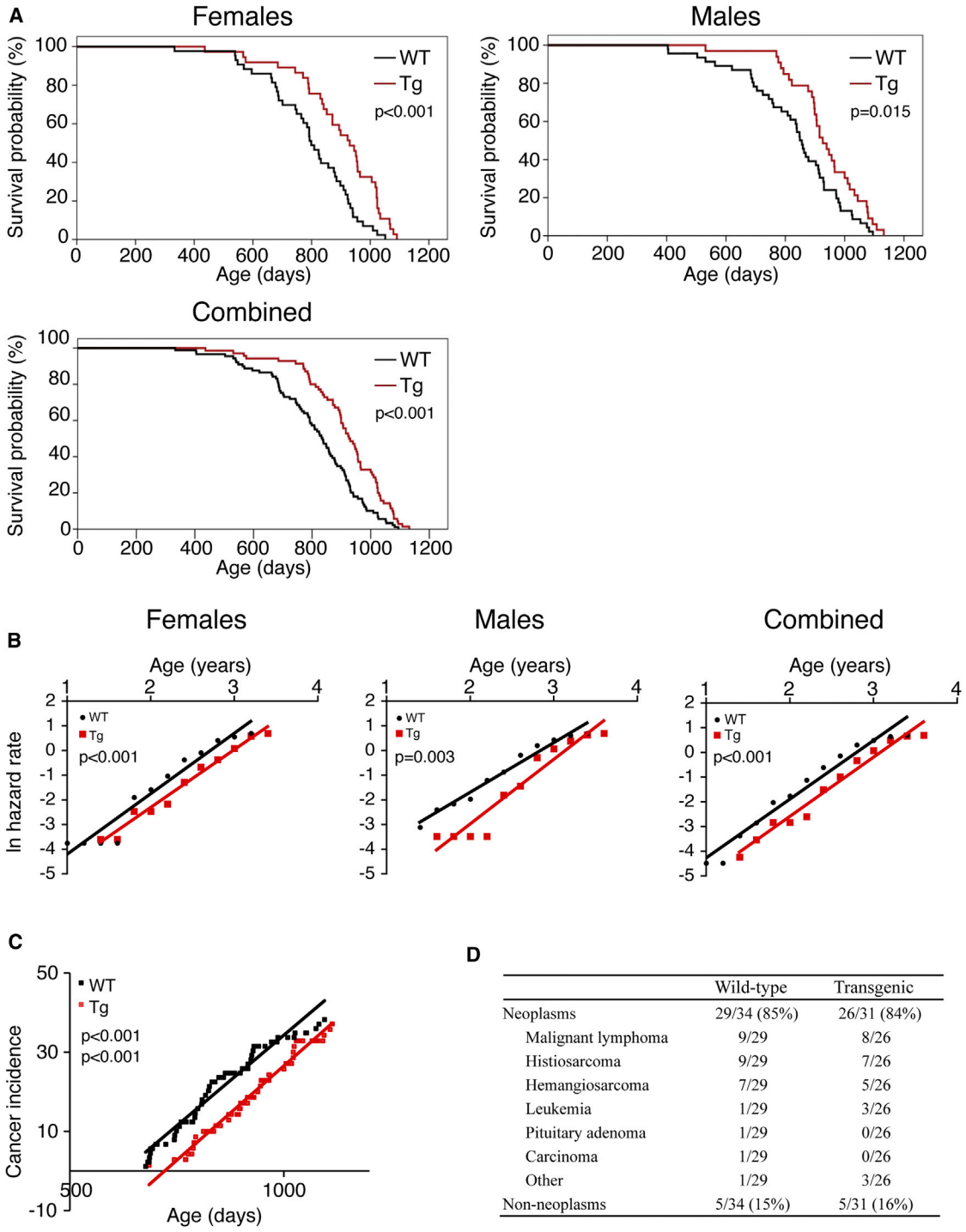

D

	Wild-type	Transgenic
Neoplasms	29/34 (85%)	26/31 (84%)
Malignant lymphoma	9/29	8/26
Histiosarcoma	9/29	7/26
Hemangiosarcoma	7/29	5/26
Leukemia	1/29	3/26
Pituitary adenoma	1/29	0/26
Carcinoma	1/29	0/26
Other	1/29	3/26
Non-neoplasms	5/34 (15%)	5/31 (16%)

Figure 1. BRASTO Mice Show the Extension of Both Median and Maximum Life Span and Delay the Age-Associated Mortality Rate and the Incidence of Cancer-Dependent Death

(A) Kaplan-Meier curves of BRASTO (Tg) and wild-type control (WT) mice in females (top left), males (top right), and combined sex (bottom left). p values shown were calculated by log rank test.

(B) Changes in age-associated mortality rate by plotting linear hazard rate in females, males, and combined sex. p values for the differences of fitted slopes (not significant) and y axis intercepts (shown in each panel) were calculated by ANCOVA between BRASTO and wild-type control mice.

(C and D) Accumulating incidents of cancer-dependent deaths (C) and identified causes of death (D) in aged BRASTO and wild-type control mice. p value (top) for the difference of the two genotypes was calculated by log rank test. p values for the differences of fitted slopes (not significant) and y axis intercepts (bottom) were calculated by ANCOVA. See also Figure S1.

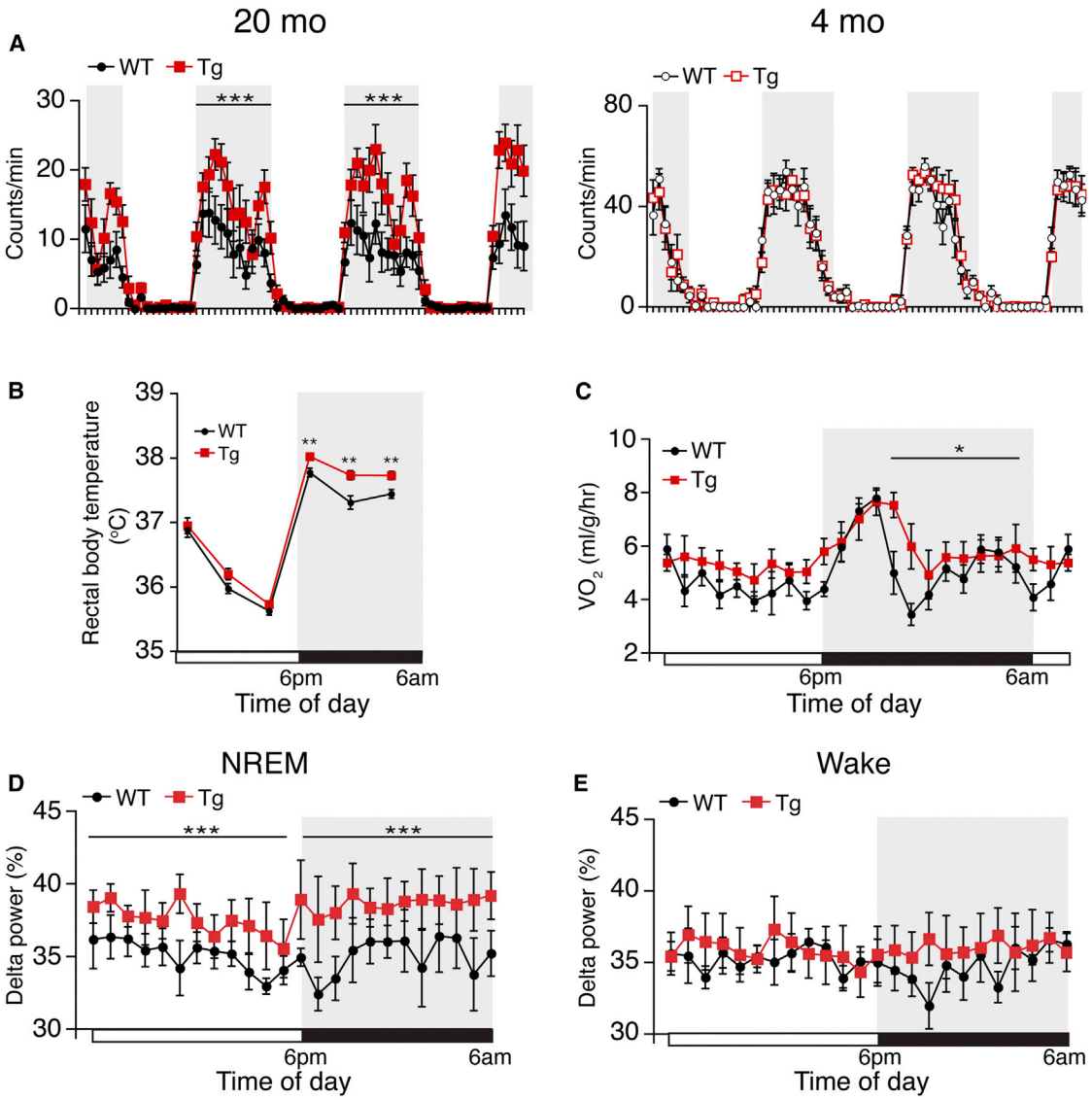

Figure 2. Aged BRASTO Mice Display Higher Physical Activity, Body Temperature, and Oxygen Consumption, and Better Quality of Sleep Compared to Wild-Type Control Mice

(A) Wheel-running activity of BRASTO (Tg) and wild-type control (WT) mice at 20 months (left) and 4 months (right) of age, respectively. Activity counts per minute at each time point are shown as mean values ± SE (***$p < 0.001$ by Wilcoxon matched-pairs singled-ranks test, n = 10–12 mice for each genotype).

(B and C) Rectal body temperature (B) and oxygen consumption (VO_2) (C) at 20 months of age. Rectal body temperature and VO_2 at each time point are shown as mean values ± SE (**$p < 0.01$ by Student's t test [B]; *$p < 0.05$ by Wilcoxon matched-pairs singled-ranks test [C, 10 p.m. to 5 a.m.], n = 10–12 mice for each genotype).

(D and E) Levels of delta power in NREM sleep (D) and wake (E) at 20 months of age. Levels of delta power at each time point are shown as mean values ± SE (***$p < 0.001$ by Wilcoxon matched-pairs singled-ranks test, n = 5–6 mice for each genotype). Shaded area represents the dark time. See also Figure S2.

during the dark time compared to age-matched control mice, whereas they showed no difference at 4 months of age (Figure 2A and Figure S2I). Twenty-month-old BRASTO mice also exhibited higher rectal body temperature and oxygen consumption, and a trend of increased energy expenditure during the dark time compared to control mice, consistent with increased nocturnal food intake in aged BRASTO mice (Figures 2B and 2C and Figures S2J and S2K). Additionally, we examined their sleep-wake patterns because of the connection between Sirt1 and orexin signaling (Panossian et al., 2011; Ramadori et al., 2011; Satoh et al., 2010). It has been reported that the delta power in non-REM (NREM) sleep, a parameter representing the quality or depth of sleep (Krueger et al., 2008), declines over age in rodents and humans (Hasan et al., 2010; Landolt et al., 1996). Intriguingly, aged BRASTO mice showed higher delta power in NREM sleep compared to control mice, whereas they showed no difference in the delta power in wake (Figures 2D and 2E), suggesting that aged BRASTO mice have better or deeper sleep. Four-month-old BRASTO and control mice showed no difference in the delta power in either NREM sleep or wake (data

not shown). Their wake and REM and NREM sleep patterns through 24 hr did not differ between young and aged BRASTO and control mice (Figure S2L and data not shown). Taken together, these findings support the notion that the onset of age-associated physiological decline is significantly delayed in aged BRASTO mice compared to age-matched control mice.

Aged BRASTO Mice Show More Youthful Mitochondrial Morphology and Function in Skeletal Muscle

To assess which tissue is possibly involved in delaying the aging process in BRASTO mice, we initially examined the expression profiles of key functional genes in white adipose tissue (WAT), brown adipose tissue (BAT), and liver. Consistent with the lack of obvious metabolic differences, we did not detect any significant changes in gene expression profiles in WAT, BAT, and liver, except for a decrease in glucose-6-phosphatase (*G6pase*) only during the dark time in the liver (Figure S3A). We also found that BAT activity, which was assessed by the diurnal expression patterns of uncoupling protein 1 (*Ucp1*) and peroxisome proliferator-activated receptor γ coactivator-1 α (*Pgc-1*α), was higher during the light time and lower during the dark time (Figure S3B), suggesting that BAT cannot be responsible for the dark time-specific enhancement in physical activity, body temperature, and oxygen consumption in aged BRASTO mice. Because skeletal muscle is another important tissue for thermogenesis in rodents, we next conducted morphometric analysis of skeletal muscle by electron microscopy between BRASTO and control mice at 20 months of age. In aged wild-type skeletal muscle, the organization of sarcomeres was often disturbed, and surrounding mitochondria were frequently absent, fused, or swollen (Figure 3A, left picture, white arrows). Strikingly, in aged BRASTO skeletal muscle, their sarcomeres were still well organized, and their mitochondria exhibited much less abnormality (Figure 3A, right picture). Consistent with these observations, the number of mitochondria was significantly higher, and their size was significantly smaller in aged BRASTO skeletal muscle compared to age-matched controls (Figure 3B). We also examined the expression of genes related to mitochondrial functions, such as *Pgc-1*α, isocitrate dehydrogenase 3α (*Idh3*α), and cytochrome *b* (*Cytb*). *Pgc-1*α expression tended to show a diurnal oscillation, showing lower expression during the light time (3 p.m.) and higher expression during the dark time (9 p.m.) in skeletal muscle. Interestingly, skeletal muscle of aged BRASTO mice showed much higher *Pgc-1*α expression during the dark time compared to control *Pgc-1*α expression during both light and dark times and BRASTO *Pgc-1*α expression during the light time (Figure 3C, left panel). The expression of *Idh3*α and *Cytb* in aged BRASTO skeletal muscle was also the highest during the dark time (Figure 3C, middle and right panels), although the difference for *Cytb* did not reach statistical significance.

In BRASTO skeletal muscle, there is no overexpression of Sirt1 (Satoh et al., 2010). Why did the skeletal muscle have more youthful morphology and function in aged BRASTO mice? We initially suspected the involvement of hormones that are known to stimulate skeletal muscle function and examined the levels of corticosterone, thyroid hormones T3 and T4, and IGF-1 in the blood during the light and dark times in aged BRASTO and control mice. There were no differences in any of these hormones between BRASTO and control mice (Figure S3C), suggesting that the observed phenotypes in aged BRASTO skeletal muscle were probably not due to hormonal changes. It has been well known that skeletal muscle receives stimulation through the sympathetic nervous system, leading to increases in the expression of β2 adrenergic receptor (*Adrb2*), a predominant subtype expressed in skeletal muscle, and cAMP levels (Lynch and Ryall, 2008). Consistent with this notion, we confirmed that *Adrb2* expression increased in skeletal muscle during the dark time in 4-month-old BRASTO and control mice (Figure 3D, left panel). The diurnal changes in *Adrb2* expression were abolished in aged wild-type skeletal muscle, whereas these changes were nicely maintained in aged BRASTO skeletal muscle (Figure 3D, right panel). cAMP levels also showed a significant increase during the dark time in aged BRASTO skeletal muscle (Figure S3D), indicating that skeletal muscle is indeed stimulated through the sympathetic nervous system in aged BRASTO mice.

Neural Activity and *Ox2r* Expression Are Significantly Enhanced in the DMH and LH during the Dark Time in Aged BRASTO Mice

The hypothalamus, particularly the DMH, has been known to regulate autonomic nervous activity. Therefore, we examined neural activity in different hypothalamic nuclei during the dark time by quantitating *cFos* expression levels. Interestingly, in the aged BRASTO hypothalamus, the DMH and LH, but not the arcuate and ventromedial hypothalamic nuclei (Arc and VMH, respectively), showed significant enhancement of *cFos* expression during the dark time compared to age-matched controls (Figure 3E). Because *Ox2r* is one of the major Sirt1 target genes in the hypothalamus (Satoh et al., 2010), we also examined the *Ox2r* expression levels during the dark time in aged BRASTO and control hypothalami. Consistent with *cFos* expression, *Ox2r* expression was significantly enhanced in the DMH and LH, but not in the Arc and VMH, in aged BRASTO mice (Figure 3F). Indeed, *Ox2r* expression showed a diurnal oscillation with higher and lower expression levels during the dark and light times, respectively (Figure S3E), consistent with the diurnal patterns of the observed BRASTO phenotypes. We also examined the expression levels of proopiomelanocortin (*Pomc*), neuropeptide Y (*Npy*), and agouti-related protein (*Agrp*) in the Arc, melanocortin-4 receptor (*Mc4r*) in the VMH, and orexin and melanin-concentrating hormone (*Mch*) in the LH. These gene expression levels did not differ between aged BRASTO and control mice (Figure S3F). Therefore, our findings suggest that neural activity in the DMH and LH is specifically enhanced during the dark time in aged BRASTO mice, possibly through the upregulation of *Ox2r* expression in these hypothalamic regions, resulting in skeletal muscle stimulation through the sympathetic nervous system.

Sirt1 Enhances *Ox2r* Promoter Activity through the Deacetylation of Nkx2-1

Because our findings indicate that the upregulation of *Ox2r* by Sirt1 in the DMH and LH might be an important mechanism for the observed phenotypes in BRASTO mice, we decided to examine how Sirt1 regulates *Ox2r* expression. In our previous study, we demonstrated that Sirt1 enhances the activity of the *Ox2r* promoter in a dose-dependent manner in cultured cells (Satoh et al., 2010). We narrowed down the Sirt1-responsive

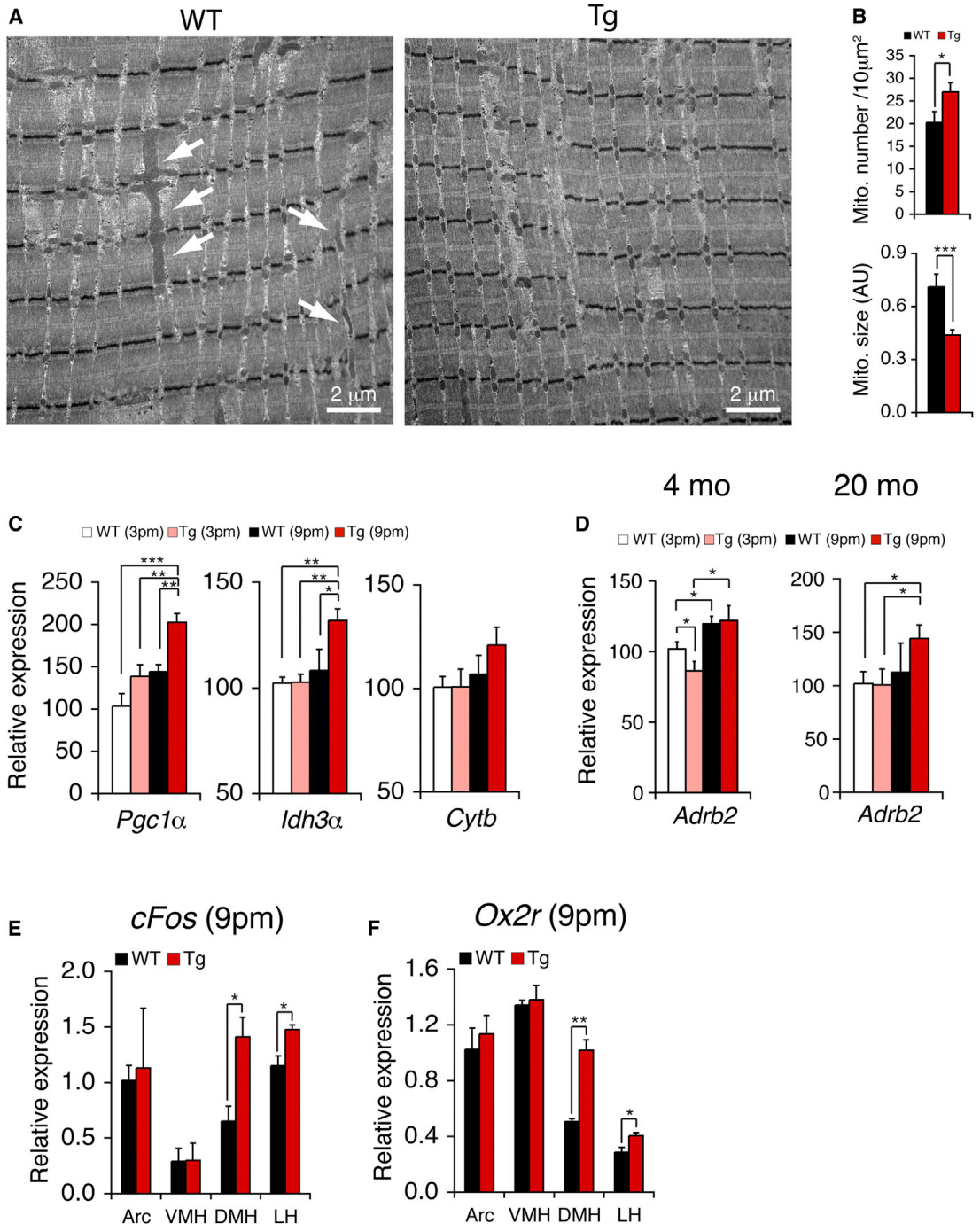

Figure 3. Aged BRASTO Mice Show More Youthful Mitochondrial Morphology and Function in Skeletal Muscle and Enhanced Neural Activation Specifically in the DMH and LH

(A and B) Morphometric analysis of the soleus muscle from aged BRASTO (Tg) and wild-type control (WT) mice. Representative electron microscope images are shown (A). The number (top) and the size (bottom) of mitochondria were measured (B), and results are shown as mean values ± SE (*$p < 0.05$, ***$p < 0.001$, n = 3 mice for each genotype, 10–15 sections per mouse).

(C and D) mRNA expression levels of genes related to skeletal muscle mitochondrial function (*Pgc1α*, *Idh3α*, and *Cytb*, C) and stimulation by the sympathetic nervous system (*Adrb2*, D) in the soleus muscle of young (D, left panel) and aged (C and D, right panel) BRASTO and wild-type control mice at 3 p.m. and 9 p.m. Each mRNA expression level was normalized to that of WT at 3 p.m. Results are shown as mean values ± SE (*$p < 0.05$, **$p < 0.01$, ***$p < 0.001$, n = 4–6 mice for each genotype).

(E and F) mRNA expression levels of *cFos* (E) and *Ox2r* (F) in the Arc, VMH, DMH, and LH of aged BRASTO and wild-type control mice at 9 p.m. Results are shown as mean values ± SE (*$p < 0.05$, **$p < 0.01$, n = 3–4 mice for each genotype). mRNA expression levels in each hypothalamic nucleus were normalized to those in the WT Arc. See also Figure S3.

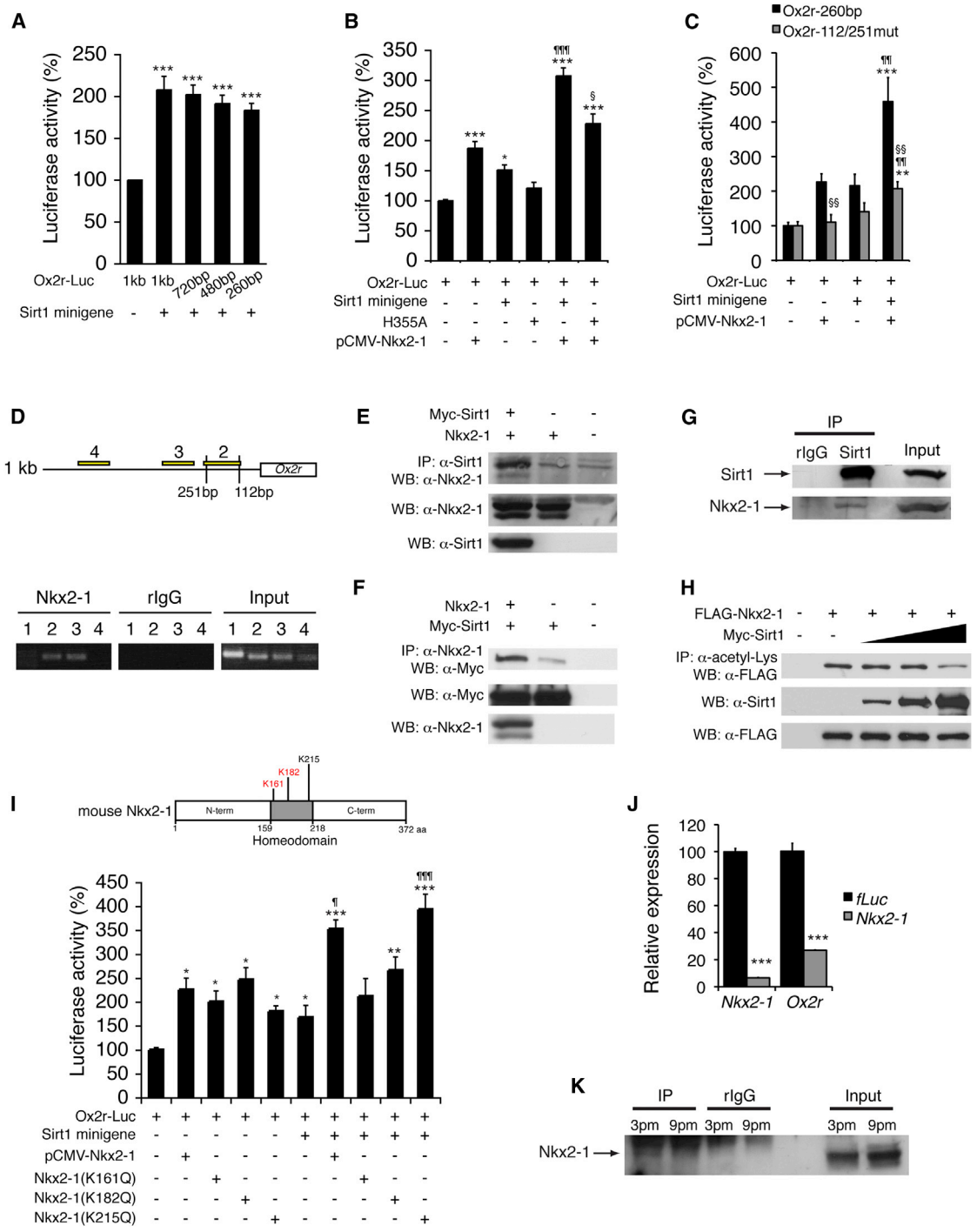

Figure 4. Sirt1 Enhances *Ox2r* Promoter Activity by Interacting with and Deacetylating a Homeodomain Transcription Factor Nkx2-1

(A–C) Luciferase activities driven by the 1 kb and truncated *Ox2r* promoter fragments (A and B, Ox2r-Luc) or the 260 bp *Ox2r* promoter or mutant carrying mutations in two Nk2 family binding sites (C, Ox2r-112/251mut) in HEK293 cells cotransfected with a Sirt1 minigene or mutant Sirt1 (H355A) (A and B) and/or Nkx2-1 (pCMV-Nkx2-1) (B and C). Luciferase activities in cells cotransfected with a backbone vector were normalized to 100%. Results are shown as mean values ± SE (control versus treatment, *p < 0.05, **p < 0.01, ***p < 0.001 by one-way ANOVA with Tukey-Kramer post hoc test [A–C]; pCMV-Nkx2-1 alone versus pCMV-Nkx2-1 with Sirt1 minigene, ¶p < 0.05, ¶¶p < 0.01, ¶¶¶p < 0.001 by Student's t test [B and C]; pCMV-Nkx2-1 with Sirt1 minigene versus pCMV-Nkx2-1 with H355A [B] or Ox2r-260bp versus Ox2r-112/251mut [C], §p < 0.05, §§p < 0.01 by Student's t test, n = 3–9).

(D) Chromatin immunoprecipitation for Nkx2-1 in the hypothalamus. Primer set 1 is designed for an unrelated genomic region. Locations of primer sets 2–4 are shown in the upper panel. Nk2 family binding sites are located at −112 and −251 positions with respect to the transcription start site in the *Ox2r* promoter.

(E–G) Coimmunoprecipitation showing the interaction of Sirt1 and Nkx2-1 overexpressed in HEK293 cells (E and F) and in the hypothalamic extracts (G).

(H) Deacetylation of Nkx2-1 by Sirt1 in HEK293 cells.

(legend continued on next page)

region from 1 kbp to 260 bp of the *Ox2r* promoter (Figure 4A). Within this 260 bp promoter region, there are two binding sites of the cAMP response element binding protein (CREB) and two binding sites of the Nk2 family of homeobox transcription factors (Figure S4). We found that the *Ox2r* promoter did not respond to CREB alone or CREB plus Sirt1 (data not shown). Among Nk2 family transcription factors, Nkx2-1 is localized in the hypothalamus in rodents (Kim et al., 2006; Mastronardi et al., 2006). An unbiased proteomic screen also suggests that Nkx2-1 could be a potential Sirt1-interacting partner (Armour et al., 2013). Therefore, we examined whether Sirt1 and Nkx2-1 cooperate to activate the *Ox2r* promoter. Sirt1 or Nkx2-1 alone was able to activate the *Ox2r* promoter, whereas the combination of Sirt1 and Nkx2-1 further enhanced the promoter activity (Figure 4B). An enzymatically deficient Sirt1 mutant H355A failed to cooperate with Nkx2-1, suggesting that Sirt1 enzymatic activity is necessary for the upregulation of the *Ox2r* promoter activity (Figure 4B). Additionally, mutating both proximal Nk2 family binding sites abolished the response to Nkx2-1 or Sirt1 alone and exhibited significant reduction in the Sirt1/Nkx2-1-dependent enhancement of the promoter activity (Figure 4C). Furthermore, hypothalamic chromatin immunoprecipitation using an Nkx2-1-specific antibody showed that Nkx2-1 localized in the proximal promoter regions containing or close to two Nk2 family binding sites (Figure 4D), the regions where Sirt1 also localizes (Satoh et al., 2010). These results suggest that Sirt1 and Nkx2-1 colocalize on Nk2 family binding sites in the 260 bp *Ox2r* proximal promoter region and cooperate to upregulate the promoter activity.

We next examined whether Sirt1 and Nkx2-1 physically interact. When overexpressing both proteins in cultured cells, we detected the reciprocal interaction between Sirt1 and Nkx2-1 (Figures 4E and 4F). We also detected the interaction between endogenous Sirt1 and Nkx2-1 in hypothalamic extracts (Figure 4G). It has been reported that K161 and K182 of the Nkx2-1 protein are acetylated in cultured cells (Yang et al., 2004). Because Sirt1 tends to interact with its deacetylation substrates, we examined whether Sirt1 deacetylates Nkx2-1. We found that increasing Sirt1 protein expression decreased the acetylation of Nkx2-1 in a dose-dependent manner (Figure 4H). We then introduced acetylation-mimicking K-to-Q mutations to K161, K182, and K215, all of which are located in the homeodomain of Nkx2-1 (Figure 4I). K161Q and K182Q mutants completely abolished the cooperativity with Sirt1, whereas the K215Q mutant was still able to upregulate *Ox2r* promoter activity with Sirt1 (Figure 4I), indicating that Sirt1 enhances the transcriptional activity of Nkx2-1 through the deacetylation of K161 and K182 in its homeodomain and upregulates *Ox2r* expression.

To confirm that Nkx2-1 is indeed involved in the regulation of *Ox2r* gene expression, we knocked down *Nkx2-1* in primary hypothalamic neurons. The expression of *Ox2r* decreased by 73% when *Nkx2-1* expression was knocked down by 94% (Figure 4J), indicating that Nkx2-1 is important for the regulation of *Ox2r* expression in hypothalamic neurons. We also found that Nkx2-1 showed less acetylation at 9 p.m. (dark time) compared to 3 p.m. (light time) (Figure 4K), consistent with the higher expression of *Ox2r* during the dark time in the hypothalamus (Figure S3E). Taken together, these results suggest that Sirt1 and Nkx2-1 cooperate to activate *Ox2r* expression in the hypothalamus during the dark time.

The Sirt1/Nkx2-1/Ox2r-Mediated Pathway Is Necessary for the Maintenance of Physical Activity, Body Temperature, Skeletal Muscle Mitochondrial Function, and Quality of Sleep

Consistent with the cooperativity between Sirt1 and Nkx2-1, we found that Sirt1 and Nkx2-1 colocalized in the DMH and LH (Figure 5A and Figure S5A). Their colocalization was more extensive in the DMH, particularly in the compact region of the DMH, where ~90% of Sirt1-positive cells were Nkx2-1 positive (Figure 5A). In the LH, ~60% of Sirt1-positive cells were Nkx2-1 positive (Figure S5A). These Sirt1/Nkx2-1 double-positive cells in the DMH were positive for NeuN, a marker for neurons, but negative for either vesicular glutamate transporter 2 or glutamate decarboxylase 1, markers for glutamatergic and GABAergic neurons, respectively (data not shown). We are currently trying to determine the identity of these Sirt1/Nkx2-1 double-positive neurons.

Because of this significant colocalization between Sirt1 and Nkx2-1 in the DMH and LH, we asked whether Sirt1, its partner Nkx2-1, and their target gene product Ox2r are necessary for any physiological phenotypes that were significantly enhanced in aged BRASTO mice. Because no Cre driver mice are available for targeting the DMH and LH, we employed stereotactic injection of shRNA lentiviruses against each gene specifically into the DMH and LH. We first conducted this experiment in 4- to 5-month-old wild-type mice. The specificity of the injection into the DMH and LH was always confirmed by the expression of GFP (Figure S5B), and the knockdown efficiency was assessed by analyzing each gene expression in each hypothalamic nucleus. *Sirt1*, *Nkx2-1*, and *Ox2r* expression was reduced by 50%–70% specifically in the DMH and LH, but not in other hypothalamic nuclei (Figure S5C). Remarkably, physical activity during the dark time was significantly reduced by knocking down *Sirt1*, *Nkx2-1*, or *Ox2r* in the DMH and LH (Figure 5B and Figure S5D). Interestingly, *Sirt1* knockdown exhibited the most extensive reduction in physical activity, whereas *Nkx2-1* and *Ox2r* knockdown showed less and almost indistinguishable reductions. We also observed similar effects in rectal body

(I) Luciferase activity of Ox2r-Luc in HEK293 cells cotransfected with a Sirt1 minigene and/or pCMV-Nkx2-1 or Nkx2-1 mutants carrying different point mutations (K161Q, K182Q, or K215Q). Results are shown as mean values ± SE (control versus treatment, *$p < 0.05$, **$p < 0.01$, ***$p < 0.001$ by one-way ANOVA with Tukey-Kramer post hoc test; pCMV-Nkx2-1 alone versus pCMV-Nkx2-1 with Sirt1 minigene or pCMV-Nkx2-1 [K215Q] alone versus pCMV-Nkx2-1 [K215Q] with Sirt1 minigene, ¶$p < 0.05$, ¶¶¶$p < 0.001$ by Student's t test, $n = 6$). These three lysines lie within the homeodomain of Nkx2-1 protein as shown in the schematic structure of Nkx2-1. Acetylated lysine residues are shown in red.

(J) mRNA expression levels of *Nkx2-1* and *Ox2r* after knockdown of *Nkx2-1* in primary hypothalamic neurons. mRNA expression levels were normalized to those in control firefly luciferase (*fLuc*) knockdown cells for each gene. Results are shown as mean value ± SE (control versus treatment, ***$p < 0.001$ by Student's t test, $n = 3$).

(K) Acetylation levels of Nkx2-1 in hypothalamic extracts at 3 p.m. (light time) and 9 p.m. (dark time). See also Figure S4.

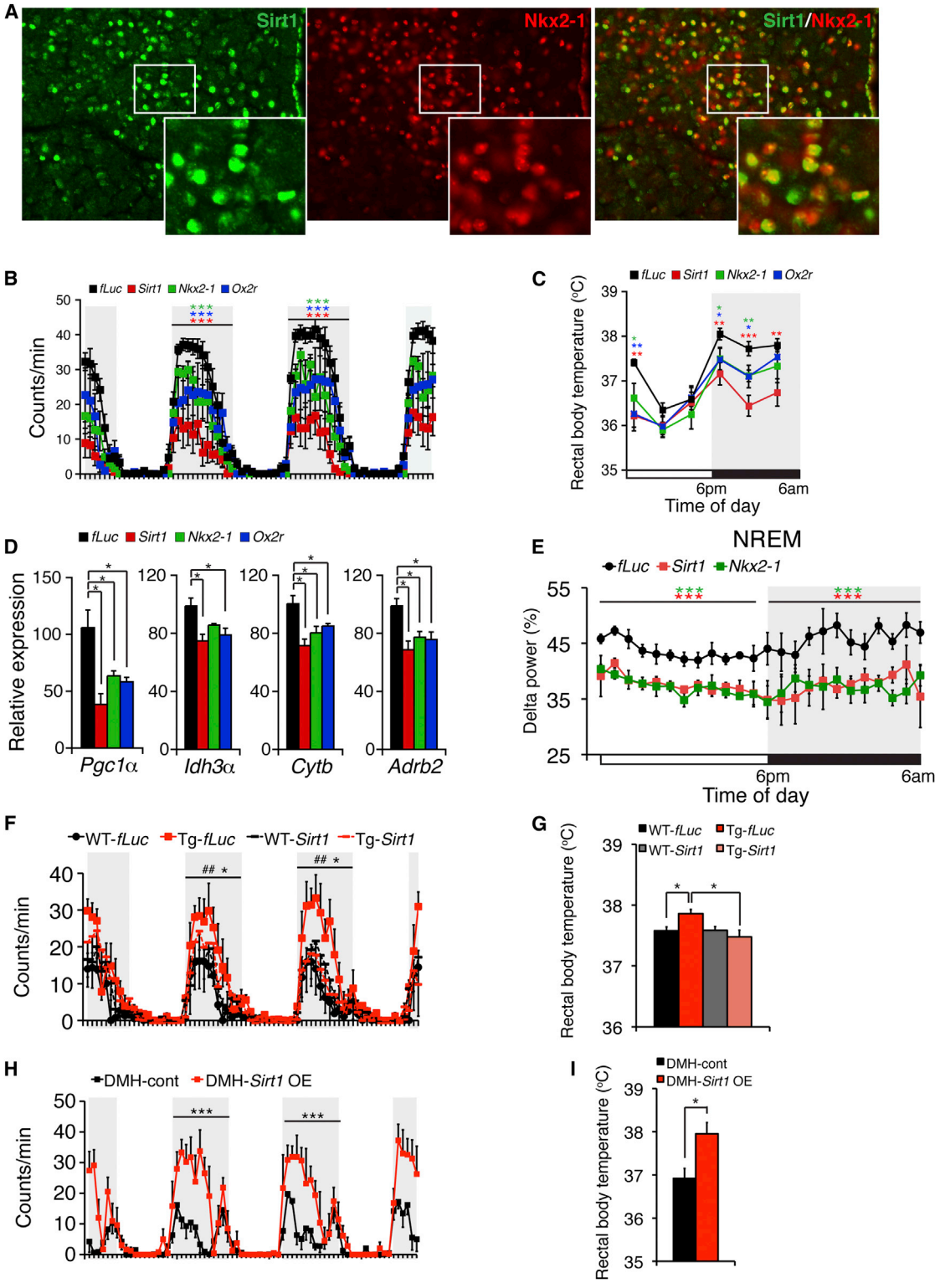

Figure 5. Sirt1, Nkx2-1, and Their Target Gene Product Ox2r in the DMH and LH Are Required to Maintain Physical Activity, Body Temperature, Skeletal Muscle Gene Expression, and Quality of Sleep during the Dark Time

(A) Immunofluorescence of Sirt1 (green), Nkx2-1 (red), and merged image (right) in the DMH. White boxes show areas that are magnified at the lower right corners of each panel.

(legend continued on next page)

temperature during the dark time (Figure 5C). Furthermore, gene expression representing skeletal muscle mitochondrial function (*Pgc-1α*, *Idh3α*, and *Cytb*) and stimulation by the sympathetic nervous system (*Adrb2*) was also significantly reduced during the dark time (Figure 5D). The delta power in NREM sleep was also significantly affected by knocking down *Sirt1* and *Nkx2-1* (Figure 5E). These results demonstrate that the molecular pathway mediated by Sirt1, Nkx2-1, and Ox2r in the DMH and LH is necessary for those physiological functions during the dark time.

To further confirm the importance of Sirt1/Ox2r signaling in the DMH and LH for age-associated BRASTO phenotypes, we next knocked down *Sirt1* and *Ox2r* specifically in the DMH and LH of 20-month-old BRASTO and control mice (Figures 5F and 5G and Figures S5E–S5H). Aged control mice showed significantly less physical activity and body temperature during the dark time compared to those in young mice, and knockdown of *Sirt1* or *Ox2r* in the DMH and LH did not show further reductions. Contrarily, in aged BRASTO mice, the DMH/LH-specific knockdown of *Sirt1* or *Ox2r* completely abolished the enhancement of physical activity and body temperature that the aged BRASTO mice with control knockdown still displayed. Additionally, DMH-specific overexpression of Sirt1 in 17- to 18-month-old wild-type B6 mice dramatically enhanced their physical activity and body temperature during the dark time to the levels comparable to those in 4- to 5-month-old B6 mice (Figures 5H and 5I). These results clearly demonstrate that the enhanced Sirt1/Ox2r signaling in the DMH and LH is critical to counteract age-associated physiological decline.

Activation of the DMH and LH and Resultant Physiological Changes Are Causally Associated with Life Span Extension in Mice

Our previous study demonstrates that Sirt1 in the DMH and LH is important for the central adaptive response to DR, a dietary regimen well known to affect aging and longevity in mammals. Results from the DMH/LH-specific stereotactic experiments further provide strong support for the causal role of Sirt1/Ox2r signaling in the DMH and LH for the significant delay in physiological phenotypes during aging. Nonetheless, in mammals, the technical difficulty of repeating life span experiments multiple times makes it very difficult to prove the strict causality of an identified mechanism for life span extension. In our case, we happened to have another line of BRASTO mice, line 1, which has much higher Sirt1 protein expression throughout the brain (Satoh et al., 2010). Indeed, *Sirt1* expression was much higher and similar through all hypothalamic nuclei in line 1 compared to line 10, whereas *Sirt1* expression levels in the DMH and LH were significantly higher compared to those in the Arc and VMH in line 10 (Figure 6A). Interestingly, in aged line 1 BRASTO mice, we found that there was no *cFos* activation in the DMH and LH during the dark time (Figure 6B). Instead, there was a significant enhancement of *cFos* activation only in the Arc in aged line 1 BRASTO mice (Figure 6B). Furthermore, the expression levels of *Pomc*, but not other neuropeptide genes, were significantly enhanced in the Arc in line 1 (Figure S6A). Therefore, in light of the results from line 10, this particular set of two BRASTO transgenic lines provided an interesting opportunity to test the tight association between neural activation in the DMH and LH and life span extension.

We conducted whole-genome sequencing for line 1 and confirmed that there were no hidden mutations or deletions, except for one synonymous homozygous single nucleotide polymorphism (data not shown). Approximately 16 tandem copies of the transgene were integrated into the region on chromosome 15 that is 0.5–1 Mbp away from the closest flanking genes (Figure S6B). No microRNAs were predicted around the integration site. Surprisingly, this line of BRASTO mice showed the life span indistinguishable from that of wild-type control mice (Figure 6C and Figure S6C). They also showed a cancer spectrum indistinguishable from that of wild-type control mice (Figure 6D). Furthermore, aged BRASTO mice in line 1 exhibited no difference in metabolic parameters (Figures S6D–S6L) and no enhancement of the physiological phenotypes that were significantly enhanced in line 10, including physical activity, rectal body temperature, and gene expression representing skeletal muscle function (Figures 6E–6G). No obvious gene expression changes were detected in BAT and liver, except for an increase in *Adrb3* in BAT that did not lead to increased cAMP levels (Figures S6M and S6N). This complete lack of age-associated phenotypes and life span extension in aged line 1 BRASTO mice shows a stark contrast to all significant phenotypes and life span extension observed in line 10 BRASTO mice, providing further strong support for our conclusion that the activation of the DMH and LH, regulated by Sirt1/Ox2r signaling, is critical to significantly delay the aging process and extend life span in mice.

DISCUSSION

Whether Sirt1 regulates aging and longevity in mammals has been a long-standing question in the field of sirtuin biology. It has already been reported that whole-body overexpression

(B and C) Wheel-running activity (B) and rectal body temperature (C) in DMH/LH-specific *Sirt1*, *Nkx2-1*, or *Ox2r* knockdown mice compared to control firefly luciferase (*fLuc*) knockdown mice. Results at each time point are shown as mean values ± SE (*p < 0.05, **p < 0.01, ***p < 0.001 by Wilcoxon matched-pairs singled-ranks test [B] or Student's t test [C], n = 6 mice for each group).

(D) mRNA expression levels of skeletal muscle genes *Pgc1α*, *Idh3α*, *Cytb*, and *Adrb2* in the soleus muscle from each knockdown mouse. Results are shown as mean values ± SE (*p < 0.05 by one-way ANOVA with Tukey-Kramer post hoc test, n = 4 mice for each group).

(E) Levels of delta power in NREM sleep. Levels of delta power at each time point are shown as mean values ± SE (***p < 0.001 by Wilcoxon matched-pairs singled-ranks test, n = 3–4 mice for each group).

(F–I) Wheel-running activity (F and H) and rectal body temperature (G and I) in DMH/LH-specific *Sirt1* knockdown compared to *fLuc* knockdown in aged BRASTO (Tg) or wild-type control (WT) mice (F and G) or DMH-specific *Sirt1* overexpression (OE) compared to control in aged B6 mice (H and I). Results at each time point are shown as mean values ± SE (Tg-*fLuc* versus WT-*fLuc*, ##p < 0.01; Tg-*fLuc* versus Tg-*Sirt1* [F] or DMH-control versus DMH-*Sirt1* OE [H], *p < 0.05, ***p < 0.001 by Wilcoxon matched-pairs singled-ranks test; *p < 0.05 by one-way ANOVA with Tukey-Kramer post hoc test [G] and Student's t test [I], n = 3–6 mice for each group). Shaded area represents the dark time. See also Figure S5.

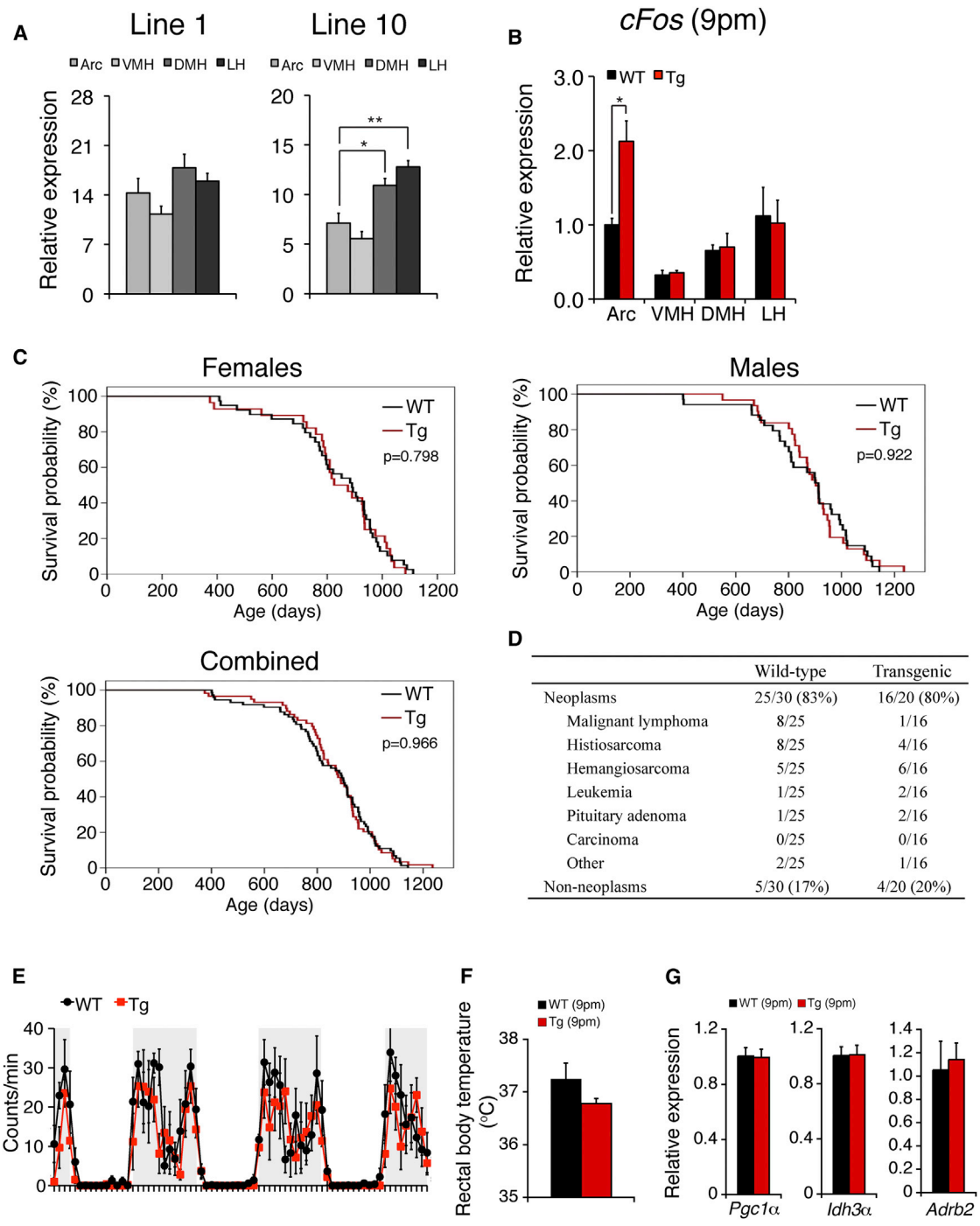

	Wild-type	Transgenic
Neoplasms	25/30 (83%)	16/20 (80%)
Malignant lymphoma	8/25	1/16
Histiosarcoma	8/25	4/16
Hemangiosarcoma	5/25	6/16
Leukemia	1/25	2/16
Pituitary adenoma	1/25	2/16
Carcinoma	0/25	0/16
Other	2/25	1/16
Non-neoplasms	5/30 (17%)	4/20 (20%)

Figure 6. Another Line of BRASTO Mice that Show Higher Sirt1 Expression through the Hypothalamus Exhibit the Complete Lack of Life Span Extension, Beneficial Physiological Phenotypes, and Activation of the DMH and LH

(A) Levels of Sirt1 mRNA in the Arc, VMH, DMH, and LH of line 1 (left) and line 10 (right) BRASTO mice. Relative expression levels were calculated as the ratio of Sirt1 mRNA in BRASTO mice versus wild-type control mice. (*$p < 0.05$, **$p < 0.01$ by one-way ANOVA with Tukey-Kramer post hoc test, n = 3 mice for each genotype).

(B) mRNA expression levels of *cFos* in the Arc, VMH, DMH, and LH at 9 p.m. Results are shown as mean values ± SE (*$p < 0.05$ by Student's t test, n = 4–6 mice for each genotype). mRNA expression levels in each hypothalamic nucleus were normalized to that in the WT Arc.

(C) Kaplan-Meier curves of line 1 BRASTO (Tg) and wild-type control (WT) mice in females (top left), males (top right), and combined sex (bottom left). p values were calculated by log rank test.

(D) Identified causes of death in aged line 1 BRASTO and wild-type control mice.

(legend continued on next page)

of Sirt1 fails to extend life span in mice (Herranz et al., 2010), leading to the conclusion that Sirt1 might not be important for the regulation of aging and longevity in mammals. The recent controversy regarding the effect of Sir2 orthologs, sir-2.1 and dSir2, on life span in worms and flies, respectively (Burnett et al., 2011), has also fueled general doubts about the role of Sir2 orthologs in aging/longevity control. On the other hand, a recent study has demonstrated that whole-body *Sirt6*-overexpressing transgenic mice show significant life span extension, although it was observed only in males (Kanfi et al., 2012).

Our present study has demonstrated that BRASTO mice, particularly the ones in line 10 that display the DMH/LH-predominant Sirt1 expression profile similar to that induced by DR, show significant life span extension and delay in aging in both males and females. Aged BRASTO mice displayed (1) significant delay in age-associated mortality and cancer-dependent death incidence; (2) significant enhancement in physical activity, body temperature, oxygen consumption, and quality of sleep; (3) more youthful structure and function in skeletal muscle; and (4) enhanced neural activation and *Ox2r* expression specifically in the DMH and LH. We have also identified Nkx2-1, a Nk2 family homeobox transcription factor, as a new partner of Sirt1 in the hypothalamus, and Sirt1 and Nkx2-1 cooperate to upregulate *Ox2r* expression during the dark time. Importantly, results from the DMH/LH-specific stereotactic experiments demonstrate that Sirt1/Ox2r signaling in the DMH and LH is responsible to counteract age-associated decline in those physiological functions. Furthermore, comparison between two independent lines of BRASTO mice reveals the tight association between the neural activation of the DMH and LH, delay in aging, and life span extension in mice.

The DMH and LH Are the Critical Areas for the Sirt1-Dependent Regulation of Aging and Longevity in Mammals

Several lines of evidence strongly indicate that the DMH and LH are the areas where Sirt1 regulates aging and longevity in mice. First, all our results from stereotactic experiments in BRASTO and wild-type mice clearly demonstrate the physiological relevance and the importance of Sirt1/Nkx2-1/Ox2r-mediated signaling in the DMH and LH for the regulation of physiological functions associated with longevity. Second, BRASTO mice in line 10 that show enhanced neural activation specifically in the DMH and LH have significantly extended life span, whereas BRASTO mice in line 1 that do not show life span extension display no enhancement of neural activity in the DMH and LH. Third, our previous study also demonstrates that Sirt1/Ox2r signaling in the DMH and LH plays an important role for the central adaptive response to DR. These findings suggest that the DMH and LH function as a "control center" for mammalian aging and longevity and that Sirt1/Nkx2-1/Ox2r-mediated signaling in the DMH and LH plays a critical role for maintaining youthful physiology and thereby mediating delay in aging and life span extension in mammals (Figure 7). This Sirt1/Nkx2-1/Ox2r-mediated pathway likely controls the sensitivity of a specific subset of DMH and LH neurons, namely Sirt1/Nkx2-1 double-positive neurons, to orexin through the regulation of *Ox2r* expression. Indeed, *Sirt1* overexpression was able to enhance the *cFos* response to orexin-B in primary hypothalamic neurons (our preliminary finding). Currently, the identity of these Sirt1/Nkx2-1 double-positive neurons is unknown. It will be of great importance to precisely characterize these Sirt1/Nkx2-1-double positive neurons, including the neurotransmitter they use.

Potential Mechanisms by which Sirt1 in the DMH and LH Counteracts Age-Associated Physiological Decline and Thereby Contributes to Life Span Extension in BRASTO Mice

How can Sirt1 in the DMH and LH mediate the effects of delaying aging and extending life span? One possible explanation is that Sirt1 mediates such beneficial effects by changing systemic metabolic parameters. However, aged BRASTO mice did not show any significant differences in metabolic phenotypes, including body weight; fed and fasted glucose, insulin, and lipid levels; and glucose and insulin tolerance. Key metabolic genes in WAT, BAT, and liver also showed no physiologically relevant changes in aged BRASTO mice. Therefore, it seems unlikely that Sirt1 mediates these beneficial effects by simply affecting systemic metabolic profiles.

Interestingly, we found that skeletal muscle maintained youthful structure and function in aged BRASTO mice. Because hormones that can stimulate skeletal muscle, including corticosterone, T3 and T4, and IGF-1, did not differ between aged BRASTO and control mice, the hypothalamus-pituitary hormonal axis does not seem to be responsible for these striking skeletal muscle phenotypes in aged BRASTO mice. Instead, aged BRASTO skeletal muscle showed significant increases in *Adrb2* expression and cAMP levels during the dark time, suggesting that skeletal muscle is stimulated through the sympathetic nervous system. The mechanism by which the signal from the hypothalamus is specifically directed to skeletal muscle still remains unknown. Nonetheless, skeletal muscle stimulated by the sympathetic nervous system might induce systemic events that contribute to the delay in aging and life span extension. Intriguingly, in flies, it has been reported that activating FOXO signaling in muscle extends life span by enhancing protein homeostasis in other tissues and inducing a systemic fasting-like response (Demontis and Perrimon, 2010). Therefore, in mammals, it is possible that skeletal muscle functions as a downstream effector that regulates the systemic process of aging in response to the neural signal coming from the hypothalamus. We are currently investigating this possibility in aged BRASTO mice.

Another interesting possibility, which is not mutually exclusive to other possibilities, is that maintaining higher delta power in NREM sleep also contributes to delay in aging and

(E and F) Wheel-running activity (E) and rectal body temperature (F) at 20 months of age. Results are shown as mean values ± SE (n = 6–8 mice for each genotype). Shaded area represents the dark time.
(G) mRNA expression levels of *Pgc1α*, *Idh3α*, and *Adrb2* in the soleus muscle of aged line 1 BRASTO mice and wild-type control mice at 9 p.m. Results are shown as mean values ± SE (n = 3 mice for each genotype). See also Figure S6.

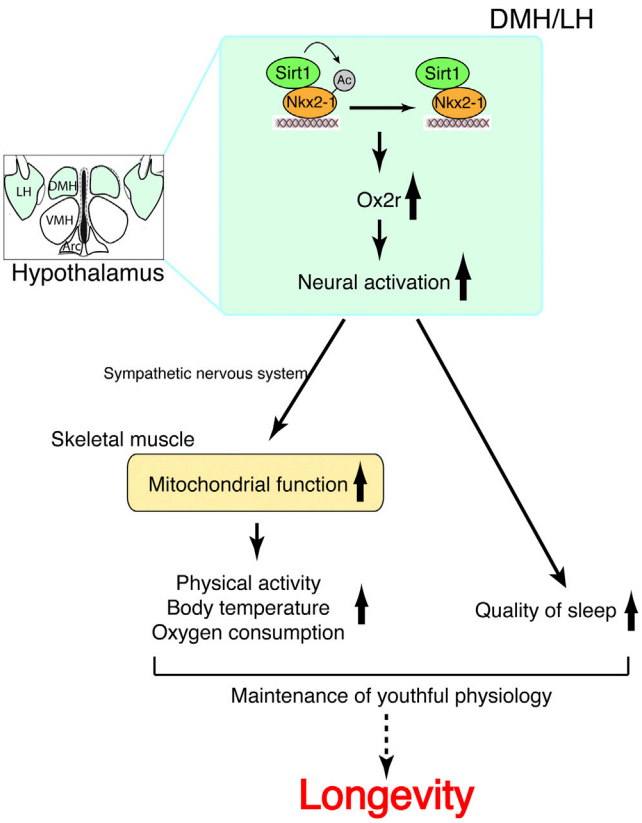

Figure 7. A Model for the Role of Hypothalamic Sirt1 in the Regulation of Aging and Longevity in Mammals

In the hypothalamus, specifically in the DMH and LH, Sirt1 upregulates *Ox2r* expression and neural activation by interacting with and deacetylating Nkx2-1. Enhanced neural activity in the DMH and LH stimulates the sympathetic nervous system and maintains skeletal muscle mitochondrial morphology and function, physical activity, body temperature, and oxygen consumption during aging. This neural activation by Sirt1/Nkx2-1/Ox2r is also critical to preserve quality of sleep during aging. These functional benefits contribute to the maintenance of youthful physiology and promote longevity.

life span extension in aged BRASTO mice. Delta power in NREM sleep, which diminishes with age in mice and humans (Hasan et al., 2010; Landolt et al., 1996), is considered a measure of sleep intensity and a reflection of sleep quality (Krueger et al., 2008). Our knockdown results show that the Sirt1/Nkx2-1/Ox2r-mediated pathway is critical to maintain delta power in NREM sleep. Because the functional connection between sleep and aging/longevity control is poorly understood, this particular finding provides an important clue to investigate the effect of sleep intensity/quality on the aging process and life span in mammals.

Implications from the Comparison of two Independent BRASTO Lines for the Role of Hypothalamic Nuclei in Aging/Longevity Control

A unique strength of our present study is that we were able to conduct the comparison between two independent transgenic lines that exhibited completely different aging/longevity phenotypes. Because whole-genome analyses assured that there were no other systemically relevant genetic changes in these two BRASTO lines, this striking phenotypic difference provides an interesting opportunity to identify major determinants in the Sirt1-dependent regulation of mammalian aging and longevity.

Given the importance of Sirt1 in the DMH and LH for the maintenance of youthful physiology, the key difference between lines 1 and 10 is probably not the difference in Sirt1 expression levels in the DMH and LH but the difference in Sirt1 in other hypothalamic nuclei, such as the Arc. Indeed, the Arc in line 1 BRASTO mice exhibits much higher neural activity during the dark time compared to controls, whereas there is no enhancement of neural activity in the DMH and LH. When the Arc is hyperactivated due to relatively high Sirt1 activity, the neural activation in the DMH and LH might be significantly suppressed, resulting in no delay of aging and no life span extension. It has previously been shown that there is a significant projection from the Arc to the DMH and LH (Bouret et al., 2004), implying the possibility that the Arc could regulate the neural activity of the DMH and LH. It will be of great interest to compare DMH/LH-specific and Arc-specific *Sirt1* overexpressors for aging and longevity phenotypes. Although further investigation will be required to test these possibilities, our findings shed new light on potential regulatory circuits within the hypothalamus that could modify the function of the DMH and LH for the regulation of aging and longevity in mammals.

CONCLUSION

Our present study demonstrates the importance of hypothalamic Sirt1 in aging/longevity control in mice. The Sirt1/Nkx2-1/Ox2r-mediated pathway in the DMH and LH stimulates skeletal muscle function via the sympathetic nervous system and maintains youthful physiology, contributing to the delay in aging and life span extension. These findings open a novel possibility that intertissue communication between the hypothalamus and peripheral tissues through the autonomic neural network plays a critical role in the regulation of aging and longevity in mammals.

EXPERIMENTAL PROCEDURES

Life Span Analysis

All animals were kept in our animal facility with free access to standard laboratory diet and water. Repeated serological tests verified that the mice housed in our suite were specific pathogen free. No mice used for the longevity study were used for any other biochemical, physiological, or metabolic tests. All mice in the aging cohorts were carefully inspected every day. The endpoint of life was the time when each mouse was found dead during daily inspection. Moribund mice were euthanized according to our institutional animal care guidelines, and the time at euthanasia was its endpoint. Survival data of each cohort were analyzed by plotting the Kaplan-Meier curve and performing the log rank test using PASW Statistics Version 18.0 (IBM). In addition to median life span, maximum 90% or 80% life span, the age at which 10% or 20% of the mice in each cohort remain alive, respectively, were compared between BRASTO and wild-type control mice for each sex using Student's t test. Necropsy was conducted immediately after death or euthanasia by the Washington University Mouse Pathology Core facility. Age-associated mortality rate (q_x) was estimated as the number of animals alive at the end of the interval over the number of animals at the start of the interval. The hazard rate (hz) was estimated by $hz = 2q_x/(2-q_x)$ (de Magalhães et al., 2005), and natural logarithm of hz was plotted. Difference between BRASTO and wild-type control mice was measured using analysis of covariance (ANCOVA).

Animal Experimentation

Assessments of both wheel-running and exploratory (vertical rearing) activities over the 24 hr periods and measurements of rectal body temperature were performed as previously described (Satoh et al., 2010). Metabolic parameters were measured using an Oxymax indirect calorimetry system (Columbus Instruments), as described previously (Yoshino et al., 2011). Details for sleep analysis and stereotactic experiments are described in the Supplemental Experimental Procedures. All animal studies were approved by the Washington University Animal Studies Committee and were in accordance with NIH guidelines.

Statistical Analysis

Differences between two groups were assessed using the Student's unpaired t test. Comparisons among several groups were performed using one-way ANOVA with the Tukey-Kramer post hoc test. Wilcoxon matched-pairs singled-ranks test was used to compare differences in physical activity, metabolic phenotypes, and delta power. $p < 0.05$ was considered statistically significant.

SUPPLEMENTAL INFORMATION

Supplemental Information includes six figures, Supplemental Experimental Procedures, and Supplemental References and can be found with this article online at http://dx.doi.org/10.1016/j.cmet.2013.07.013. The whole-genome sequencing data for two BRASTO transgenic lines are available at the following archive site: http://cgs.wustl.edu/solexa/Imai_0619/. To open the files, a genome viewer such as the Integrative Genomics View (IGV; http://www.broadinstitute.org/igv/) is required.

ACKNOWLEDGMENTS

We thank Myeong Jin Yoon, Daniel Granados-Fuentes, Tatsiana Simon, Sara Conyers, Trey Coleman, Suellen Greco, Jin-Moo Lee, Ronaldo Perez, Mingjie Lee, Nada Husic, and Karen Green for their technical help, and members of the Imai laboratory for their help and discussions. This work was supported by grants from the National Institute on Aging (AG024150, AG037457) and the Ellison Medical Foundation (to S.I.) and the National Institute of Mental Health (MH063104) (to E.D.H.). A.S. was supported by the JSPS Postdoctoral Fellowship for Research Abroad. S.I. served as a scientific advisory board member for Sirtris, a GSK company.

Received: February 4, 2013
Revised: July 5, 2013
Accepted: July 31, 2013
Published: September 3, 2013

REFERENCES

Armour, S.M., Bennett, E.J., Braun, C.R., Zhang, X.Y., McMahon, S.B., Gygi, S.P., Harper, J.W., and Sinclair, D.A. (2013). A high-confidence interaction map identifies SIRT1 as a mediator of acetylation of USP22 and the SAGA coactivator complex. Mol. Cell. Biol. *33*, 1487–1502.

Banks, A.S., Kon, N., Knight, C., Matsumoto, M., Gutiérrez-Juárez, R., Rossetti, L., Gu, W., and Accili, D. (2008). SirT1 gain of function increases energy efficiency and prevents diabetes in mice. Cell Metab. *8*, 333–341.

Bartke, A. (2011). Pleiotropic effects of growth hormone signaling in aging. Trends Endocrinol. Metab. *22*, 437–442.

Bordone, L., Cohen, D., Robinson, A., Motta, M.C., van Veen, E., Czopik, A., Steele, A.D., Crowe, H., Marmor, S., Luo, J., et al. (2007). SIRT1 transgenic mice show phenotypes resembling calorie restriction. Aging Cell *6*, 759–767.

Bouret, S.G., Draper, S.J., and Simerly, R.B. (2004). Formation of projection pathways from the arcuate nucleus of the hypothalamus to hypothalamic regions implicated in the neural control of feeding behavior in mice. J. Neurosci. *24*, 2797–2805.

Burnett, C., Valentini, S., Cabreiro, F., Goss, M., Somogyvári, M., Piper, M.D., Hoddinott, M., Sutphin, G.L., Leko, V., McElwee, J.J., et al. (2011). Absence of effects of Sir2 overexpression on lifespan in *C. elegans* and *Drosophila*. Nature *477*, 482–485.

Chen, D., Steele, A.D., Lindquist, S., and Guarente, L. (2005). Increase in activity during calorie restriction requires Sirt1. Science *310*, 1641.

Cohen, D.E., Supinski, A.M., Bonkowski, M.S., Donmez, G., and Guarente, L.P. (2009). Neuronal SIRT1 regulates endocrine and behavioral responses to calorie restriction. Genes Dev. *23*, 2812–2817.

de Magalhães, J.P., Cabral, J.A., and Magalhães, D. (2005). The influence of genes on the aging process of mice: a statistical assessment of the genetics of aging. Genetics *169*, 265–274.

Demontis, F., and Perrimon, N. (2010). FOXO/4E-BP signaling in *Drosophila* muscles regulates organism-wide proteostasis during aging. Cell *143*, 813–825.

Durieux, J., Wolff, S., and Dillin, A. (2011). The cell-non-autonomous nature of electron transport chain-mediated longevity. Cell *144*, 79–91.

Feldman, J.L., Dittenhafer-Reed, K.E., and Denu, J.M. (2012). Sirtuin catalysis and regulation. J. Biol. Chem. *287*, 42419–42427.

Haigis, M.C., and Sinclair, D.A. (2010). Mammalian sirtuins: biological insights and disease relevance. Annu. Rev. Pathol. *5*, 253–295.

Hasan, S., Dauvilliers, Y., Mongrain, V., Franken, P., and Tafti, M. (2010). Age-related changes in sleep in inbred mice are genotype dependent. Neurobiol. Aging *33*, http://dx.doi.org/10.1016/j.neurobiolaging.2010.05.010, 195e13-26.

Herranz, D., Muñoz-Martin, M., Cañamero, M., Mulero, F., Martinez-Pastor, B., Fernandez-Capetillo, O., and Serrano, M. (2010). Sirt1 improves healthy ageing and protects from metabolic syndrome-associated cancer. Nat. Commun. *1*, 3.

Kanfi, Y., Naiman, S., Amir, G., Peshti, V., Zinman, G., Nahum, L., Bar-Joseph, Z., and Cohen, H.Y. (2012). The sirtuin SIRT6 regulates lifespan in male mice. Nature *483*, 218–221.

Kenyon, C.J. (2010). The genetics of ageing. Nature *464*, 504–512.

Kim, J.G., Nam-Goong, I.S., Yun, C.H., Jeong, J.K., Kim, E.S., Park, J.J., Lee, Y.C., Kim, Y.I., and Lee, B.J. (2006). TTF-1, a homeodomain-containing transcription factor, regulates feeding behavior in the rat hypothalamus. Biochem. Biophys. Res. Commun. *349*, 969–975.

Krueger, J.M., Rector, D.M., Roy, S., Van Dongen, H.P., Belenky, G., and Panksepp, J. (2008). Sleep as a fundamental property of neuronal assemblies. Nat. Rev. Neurosci. *9*, 910–919.

Kume, S., Uzu, T., Horiike, K., Chin-Kanasaki, M., Isshiki, K., Araki, S., Sugimoto, T., Haneda, M., Kashiwagi, A., and Koya, D. (2010). Calorie restriction enhances cell adaptation to hypoxia through Sirt1-dependent mitochondrial autophagy in mouse aged kidney. J. Clin. Invest. *120*, 1043–1055.

Landolt, H.P., Dijk, D.J., Achermann, P., and Borbély, A.A. (1996). Effect of age on the sleep EEG: slow-wave activity and spindle frequency activity in young and middle-aged men. Brain Res. *738*, 205–212.

Lynch, G.S., and Ryall, J.G. (2008). Role of beta-adrenoceptor signaling in skeletal muscle: implications for muscle wasting and disease. Physiol. Rev. *88*, 729–767.

Mastronardi, C., Smiley, G.G., Raber, J., Kusakabe, T., Kawaguchi, A., Matagne, V., Dietzel, A., Heger, S., Mungenast, A.E., Cabrera, R., et al. (2006). Deletion of the Ttf1 gene in differentiated neurons disrupts female reproduction without impairing basal ganglia function. J. Neurosci. *26*, 13167–13179.

Panossian, L., Fenik, P., Zhu, Y., Zhan, G., McBurney, M.W., and Veasey, S. (2011). SIRT1 regulation of wakefulness and senescence-like phenotype in wake neurons. J. Neurosci. *31*, 4025–4036.

Pfluger, P.T., Herranz, D., Velasco-Miguel, S., Serrano, M., and Tschöp, M.H. (2008). Sirt1 protects against high-fat diet-induced metabolic damage. Proc. Natl. Acad. Sci. USA *105*, 9793–9798.

Ramadori, G., Fujikawa, T., Anderson, J., Berglund, E.D., Frazao, R., Michán, S., Vianna, C.R., Sinclair, D.A., Elias, C.F., and Coppari, R. (2011). SIRT1 deacetylase in SF1 neurons protects against metabolic imbalance. Cell Metab. *14*, 301–312.

Satoh, A., Brace, C.S., Ben-Josef, G., West, T., Wozniak, D.F., Holtzman, D.M., Herzog, E.D., and Imai, S. (2010). SIRT1 promotes the central adaptive response to diet restriction through activation of the dorsomedial and lateral nuclei of the hypothalamus. J. Neurosci. *30*, 10220–10232.

Wang, H., Zhang, P., and Wang, C.T. (2009). [Analysis of expression pattern of a novel testis-highly expressed gene Biot2-L and the primary study on its role in testis development]. Sichuan Da Xue Xue Bao Yi Xue Ban *40*, 853–856.

Yang, L., Yan, D., Bruggeman, M., Du, H., and Yan, C. (2004). Mutation of a lysine residue in a homeodomain generates dominant negative thyroid transcription factor 1. Biochemistry *43*, 12489–12497.

Yoshino, J., Mills, K.F., Yoon, M.J., and Imai, S. (2011). Nicotinamide mononucleotide, a key NAD(+) intermediate, treats the pathophysiology of diet- and age-induced diabetes in mice. Cell Metab. *14*, 528–536.

Zhang, G., Li, J., Purkayastha, S., Tang, Y., Zhang, H., Yin, Y., Li, B., Liu, G., and Cai, D. (2013). Hypothalamic programming of systemic ageing involving IKK-β, NF-κB and GnRH. Nature *497*, 211–216.

Zoncu, R., Efeyan, A., and Sabatini, D.M. (2011). mTOR: from growth signal integration to cancer, diabetes and ageing. Nat. Rev. Mol. Cell Biol. *12*, 21–35.